Thermal Spray 2013—Innovative Coating Solutions for the Global Economy
Proceedings of the International Thermal Spray Conference
May 13–15, 2013, Busan, Republic of Korea
R.S. Lima, A. Agarwal, M.M. Hyland, Y.-C. Lau, G. Mauer, A. McDonald, F.-L. Toma, editors

Copyright © 2013 ASM International®
All rights reserved
www.asminternational.org

Tungsten Carbide Deposition Processes for Hard Chrome Alternative: Preliminary Study of HVAF vs. HVOF Thermal Spray Processes

C. Lyphout
University West, Production Technology West, Trollhättan, SWEDEN
**E-mail: christophe.lyphout@hv.se*

J. Kitamura, K. Sato, J. Yamada
Fujimi Incorporated, JAPAN

S. Dizdar
Höganäs Sweden AB, SWEDEN

Abstract

Electrolytic Hard Chrome (EHC) method, which is still widely utilized in the printing, automotive and off-shore industries, is coming to be subjected to strong restrictions in the next decade in the use of hexavalent Chromium, with the increasing strengthening of European normative. Alternative methods to EHC, such as High Kinetic Thermal Spray Technology, have shown a growing interest the past decades. Compared to conventional HVOF processes which pioneered the development of WC-based coated materials, newly developed HVAF systems are processing at higher kinetic energy and more particularly at lower temperature, which significantly reduces feedstock oxidation and decarburization, then increasing respective wear and corrosion resistance properties. A preliminary investigation of HVOF- and HVAF-sprayed coatings is here proposed on the evaluation basis of material decarburization, coating porosity and microhardness. Role of carbides size and morphology on coating adhesion strength, wear and corrosion resistance properties are preliminary discussed.

Introduction

Surface Technology is a key technology to add functionality to surfaces components and enhance the lifetime of the materials compared to structural mechanisms of breakdown owing to corrosion and wear environments. In the field of wear, erosion and corrosion applications, recent restrictions in the use of hexavalent form of chrome element has driven the need of replacing Electrolyte Hard Chrome plating (EHC) by other material/process with equivalent tribological properties (Ref 1). Low temperature high kinetic thermal spray processes emerge as an interesting and promising alternative method to EHC (Ref 2). The past decades, HVOF solutions for spraying state-of-the-art coatings of WC-Co-Cr 86/10/4 (Ref 3-7) and Cr_3C_2-NiCr 75/25 (Ref 7-10) materials have been largely developed, as an alternative to conventional Ni-based coatings. The need to evaluate the potentialities of HVOF spraying, as well as its limitations in spraying such materials is essential to understand why newly-developed technologies, such as High Velocity Air Fuel (HVAF), Cold Gas Dynamic Spray (CGDS), and more recently High Velocity Suspension Flame Spraying (HVSFS), are gaining interest nowadays as an alternative to HVOF spraying. Compared to conventional spraying techniques, WC-Co cermet have been deposited the past decades by HVOF, owing to higher velocities and lower temperatures which result in less decomposition and/or decarburization of the WC elements during spraying (Ref 7), reducing the amount of undesirable phases such as W_2C, W, and amorphous or nanocrystalline Co-W-C phase (Ref 11, 12). Through the past decade, a certain amount of studies have been published on different HVOF gun design, such as JP5000 (Ref 3,5,6,7), Warm Spray (Ref 13), DJ2700/2600 (Ref 4,7), JetKote II (Ref 14,15), CJS (Ref 4) and K2 (Ref 15). While lowering the process temperature appears to be the solution to suppress decarburization and decomposition of WC phases, Jacob et al. successfully deposited WC-Co and WC-Co-Cr coatings using High-Velocity Air Fuel (HVAF) process (Ref 16) showing no detrimental phase from decomposition or oxidation during deposition, and resulting in higher hardness and wear resistance. Improvement of HVAF gun performances over the past few years have now led to the emergence of commercial systems, from HVAF-Aerospray (Browning, US), AC-HVAF (Kermetico) to up-to-date HVAF-M2 and HVAF-M3, also referenced as Supersonic Air Fuel SAF (UniqueCoat Technology, US).

A comparative study of HVOF-JP5000 versus HVAF-M3 sprayed coatings is here proposed on the evaluation basis of material decarburization, coating porosity and microhardness. Role of primary carbides grain size and morphology on coating dry abrasion wear and corrosion resistance properties are preliminary discussed. The present investigation is part of a broader joint collaboration between University West and Fujimi Incorporated to investigate the influence of primary carbides grain size on different wear mechanisms and corrosion resistance of the coating.

Experimental Procedure

Materials and Spray Processes

Two Tungsten carbide powders with Co matrix (Tab.1) and two tungsten carbide powders with Co-Cr matrix (Fujimi Incorporated, Japan) were sprayed utilizing the HVAF-M3 process (UniqueCoat, US) and the HVOF-JP5000 (Praxair). Domex355 steel substrates were sprayed to a targeted coating thickness of 380 microns. EHC reference was introduced in this study for corrosion resistance comparison only.

Table 1: Samples matrix of investigated processes/materials

Ref./Material	Ref./ Process	Composition	Part. size
K1 / DTS-W666	**P1**/HVAF-M3	WC-Co 88/12	-30+5 mm
K2 / DTS-W617	**P2**/HVOF-JP5000	WC-Co 88/12	-45+15 mm
K4 / DTS-W648	**P1**-HVAF-M3	WC-Co-Cr 86/10/4	-30+5 mm
K5 / DTS-W618	**P2**/HVOF-JP5000	WC-Co-Cr 86/10/4	-45+15 mm
EHC	Electrolytic plating reference		

Characterization Methods

Microstructure: Coating cross sections were analysed utilizing a Scanning Electron Microscope Table top Micrograph (Hitachi TM3000) with acceleration voltage of 15 kV. A specially designed image Analysis procedure, utilizing Aphelion software coupled with Matlab, was developed to evaluate coating porosity, primary carbides grain size (CGS) and contiguity (CC), and mean free path (MFP) distributions.
Phase Analysis: X-Ray Diffraction analysis of powder feedstock and coated systems were carried out using an Ultima IV diffractometer, Rigaku Corporation (20kv/10 mA).
Micro Hardness: Vickers Microhardness HV0.3 of the coatings was measured according to the standard ASTM E-384-10. Measurements were carried out on the polished cross-section of the coating according to ASTM E384-10 with a Vickers indenter at a load of 300 g (2,942 N) and dwell time of 15 seconds, using a Shimadzu Microhardness Tester (Tab 4). 20 impressions were made on each coating that distributed evenly in a half circle of the entire test panel.
Adhesion Strength: Coating adhesion strength was measured according to the ASTM C633-79 standard, utilizing FM1000 polymer-based media. The tests were conducted on a ZWICK Z100 tensile test machine at a speed of 0.1 mm/min.
Wear Resistance: Suga Abrasion test was conducted according to ASTM D6037 to investigate abrasive wear resistance of the coating (Fig 1-a). Dry sand rubber wheel, DSRW, abrasion wear testing was conducted according to the ASTM G65 (Fig 1-b). Additional blast erosion test was carried out to evaluate erosive wear resistance, utilizing Alumina blast media F240 (60 microns) under pressure of 0.6 MPa, at a blast angle and distance of 20° and 100 mm respectively.
Corrosion Resistance: Cyclic corrosion salt spray test was carried out according to ISO 16701, utilizing ASCOTT CC450XP equipment (Fig 1-c). Sprayed samples were polished to a Ra of 0.1, and exposed to a maximal period of six weeks (1000 hours), without additional corrosion protection on the exposed area, excepted on samples edges.

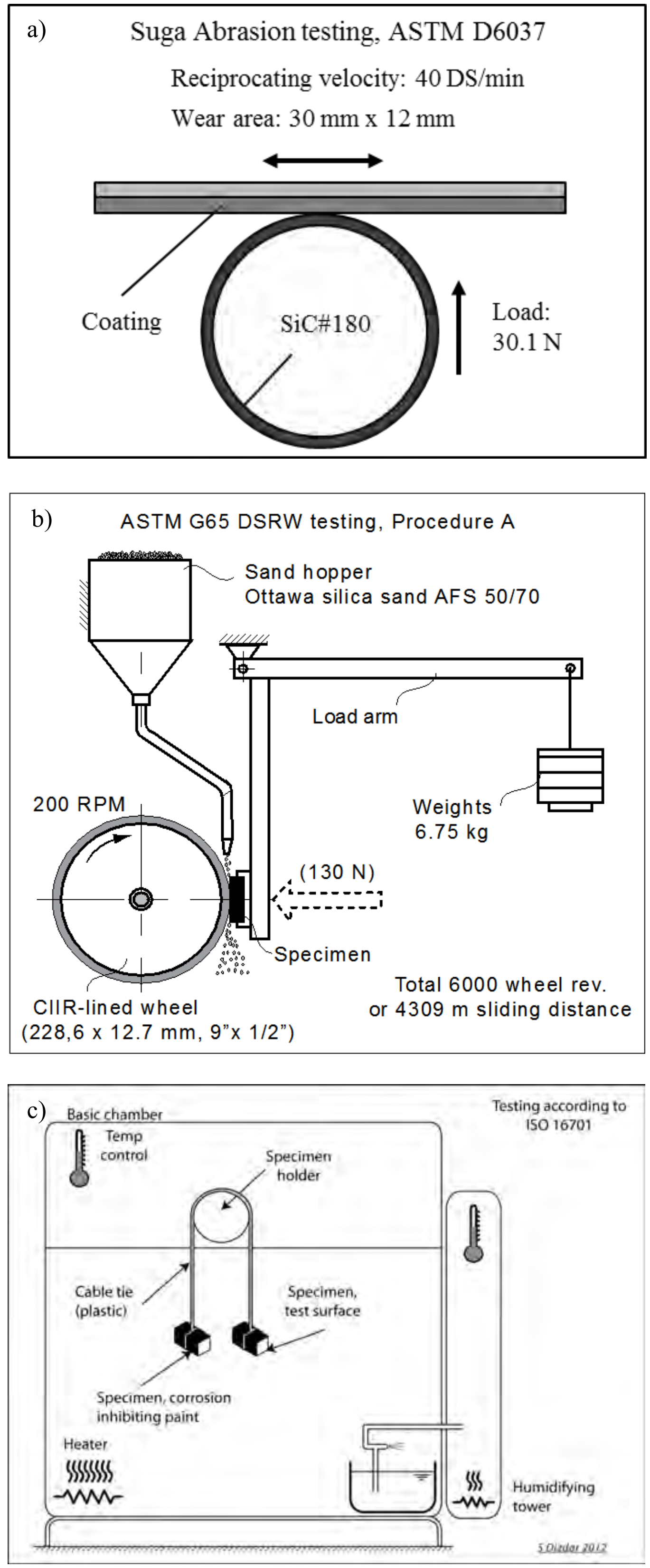

Figure 1: Wear resistance tests: a) ASTM D6037, b) ASTM G65 and c) cyclic corrosion test according to ISO 16701.

Results and Discussions

Microstructure

HVAF coatings exhibit lower porosity (Tab 2) and finer carbides size than HVOF coatings for respective powder composition (Fig 2). In order to emphasize the high frequency of extremely fine primary carbides, Image Analysis utilizing Aphelion® software was performed on one cross-section for each sample over 20 evenly distributed fields from SEM micrographs (x7000) with dimension of 1280 x 960 pixels. Each field has been binarized by thresholding functions to identify the volume fraction of porosity, carbides and matrix. Each carbide particle has been associated to an object (Fig 3) whose surface area was used to compute an Equivalent carbide diameter, as well as the intercept length and distance between carbides. Respective distributions have been evaluated (Fig 4), and weighted mean computed for the Carbide Grain Size (CGS), Carbides Contiguity (CC) and Mean Free Path (MFP).

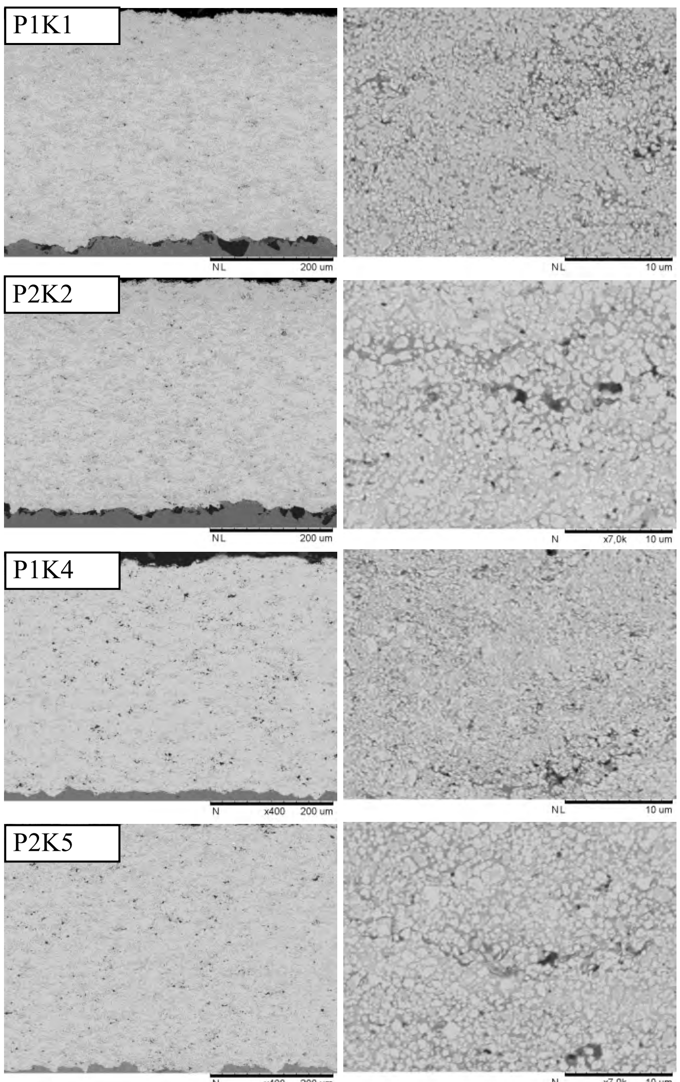

Figure 2: SEM micrographs of respective coating cross sections (X400- left; X7000-right)

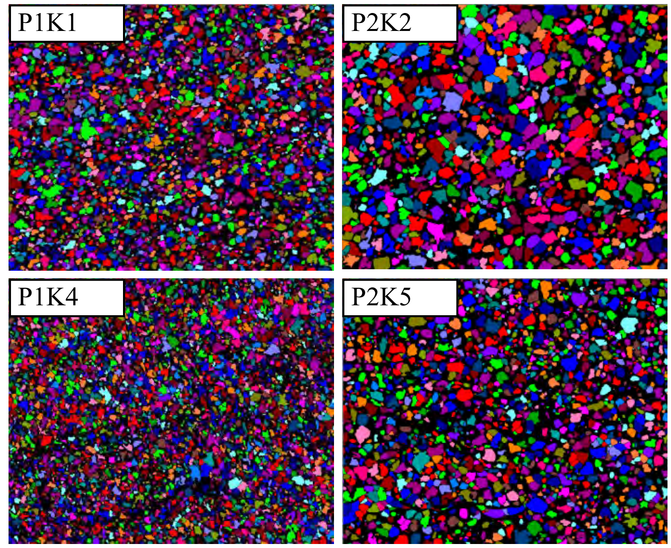

Figure 3: Clusters of carbides associated to objects through one of the 20 studied fields (X7000) for each coating

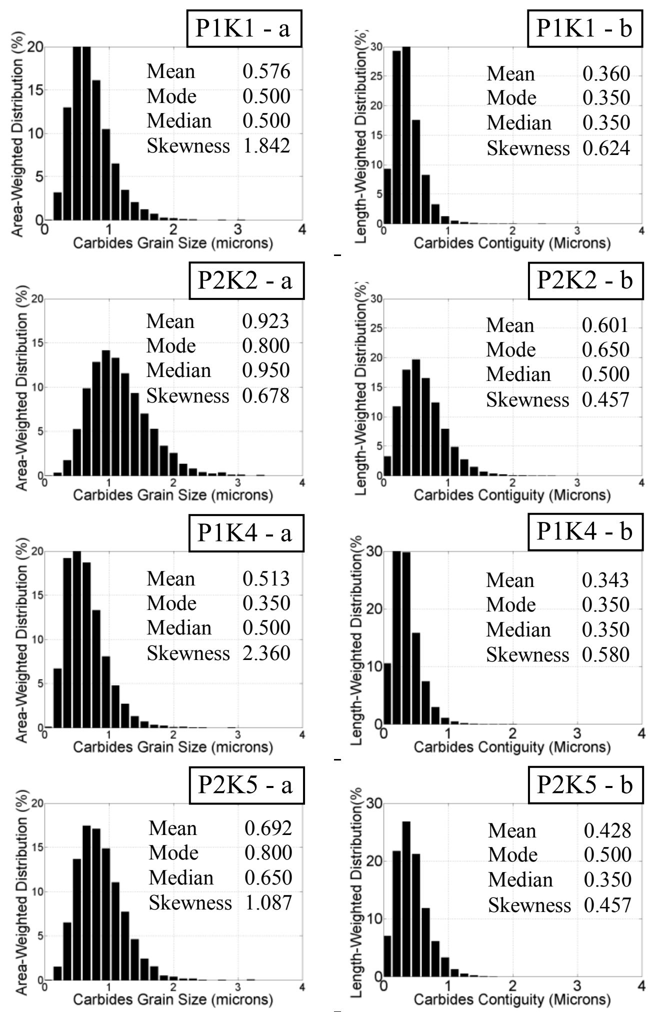

Figure 4: Respective weighted distributions of a) Carbides Grain Size (CGS) and b) Carbides Contiguity (CC)

Primary carbides sprayed with HVOF (Fig 4) exhibit coarser grain size and broader weighted distributions, the latest evaluated by a Minitab® routine. Narrower distributions of homogeneous and finer carbides in HVAF coatings lead to relative lower Mean Free Path (Tab 2), calculated from weighted averages of CGS and CC, following stereological principles (Ref 16-18) similar to the intercept analysis method.

Phase Analysis

XRD patterns of initial powders were recorded and respective phases identified (Fig 5-a). Phases W_2C and W derived from thermal decomposition of the powder during spraying were found predominantly in the HVOF-sprayed coatings compared to the HVAF-sprayed deposits (Fig 5-b). The relative absence of Co phase in HVOF coatings indicates the formation of oxides, likely CoO or Cr_3C_2CoO. Both results confirm the colder conditions observed in HVAF compared to HVOF.

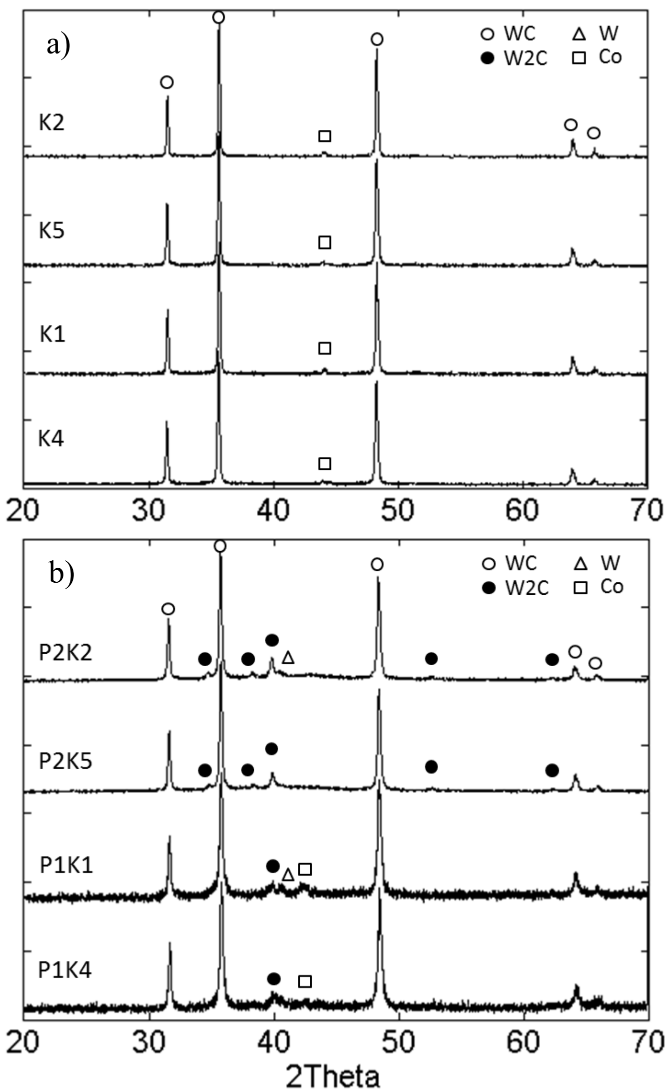

Figure 5: XRD patterns of powders (a) and coatings (b) with identification of principal phases

Table 2: CGS, CC and MFP coatings microstructure features

Image Analysis	P1K1	P2K2	P1K4	P2K5
Porosity (%)	0.5 ± 0.2	1.4 ± 0.8	0.7 ± 0.4	1.2 ± 0.8
Carbides (%)	57.7 ± 6.5	61.0 ± 5.6	55.1± 9.0	50.9 ± 2.7
CGS (μm)	0.58±0.26	0.92±0.37	0.51±0.25	0.69±0.29
CC (μm)	0.36±0.21	0.60±0.33	0.34±0.21	0.43±0.24
MFP (μm)	0.19±0.02	0.26±0.03	0.17±0.03	0.28±0.02

Adhesion Strength

No coating/substrate interface failures were observed carrying out the standard ASTM C633-79, meaning that all coatings have equivalent high adhesion strength, superior to the cohesive strength of the FM1000 glue. However different glue failure modes were observed between HVOF- and HVAF-sprayed coatings. Surface roughness and coating porosity could explain the different glue failure modes encountered. Compared to HVAF coatings, higher surface roughness and higher porosity of HVOF-sprayed deposits hindered good contact between glue and coatings, resulting in a mixed failure mode 50% in Epoxy and 50% for P2K2 and P2K5 (Tab.3).

Table 3: Coating roughness and adhesion strength

	P1K1	P2K2	P1K4	P2K5
Ra (μm)	3.7 ± 0.4	3.9 ± 0.4	3.8 ± 0.2	3.9 ± 0.4
Rz (μm)	21.5 ± 1.6	21.8 ± 1.9	21.0 ± 1.2	22.2 ± 2.0
Adhesion (MPa)	90.7 ± 5.1	78.8 ± 1.5	91.6 ± 4.0	83.6 ± 5.4
Failure mode	Epoxy	Mixed	Epoxy	Mixed

Wear Resistance

Dry wear abrasive tests performed in this study showed that HVOF-sprayed coatings exhibited significant higher dry wear resistance than HVAF-sprayed ones (Fig 6-7) for respective feedstock materials. Since no significant difference has been measured in respective coatings microhardness (Tab 4), the later cannot explain any longer the difference in wear behaviours. Despite the presence of brittle W_2C phase in HVOF coatings, other key-factors such as higher binder Mean Free Path (Tab 2) and coarser primary carbides can modify the wear mechanisms and thus compensate the volume wear loss obtained in respective dry abrasion tests (Fig 6-7).

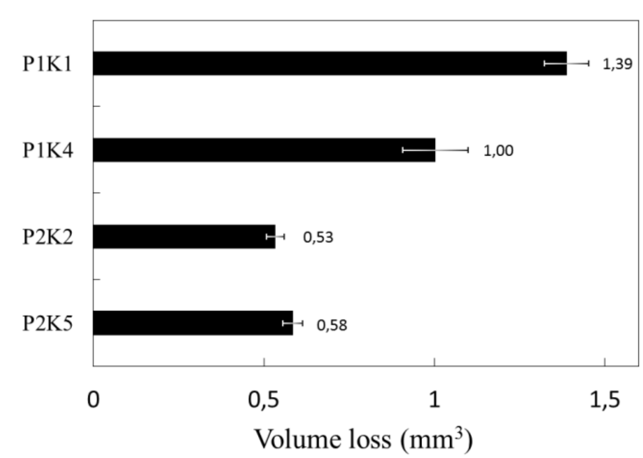

Figure 6: Volume weight loss – ASTM D6037

Table 4: ASTM E384-10 for Microhardness evaluation

HV0.3	P1K1	P2K2	P1K4	P2K5
Max	1306.5	1249.8	1342.2	1342.4
Min	772.5	904.51	859.1	822.9
Mean	1030.1	1093.0	1109.8	1077.9
Stdev	107.86	106.64	147.24	159.32

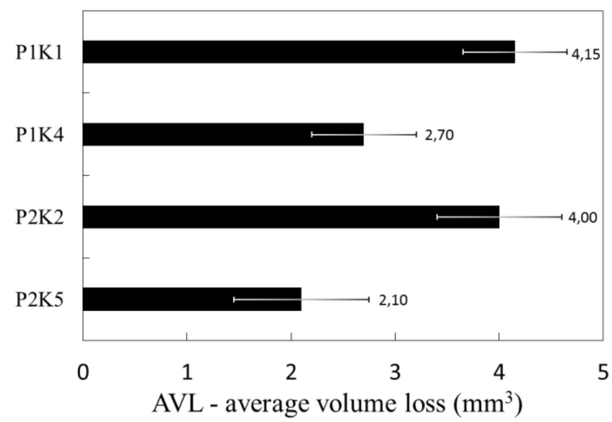

Figure 7: Volume weight loss – ASTM G65 (to be updated)

Blast Erosion results (Fig 8) also confirmed that HVOF-sprayed coatings exhibit higher erosion resistance than HVAF ones. The erosion quotient is here calculated as the ratio of the time needed to blast a certain quantity of media to the erosion depth (expressed in thousands of an inch).

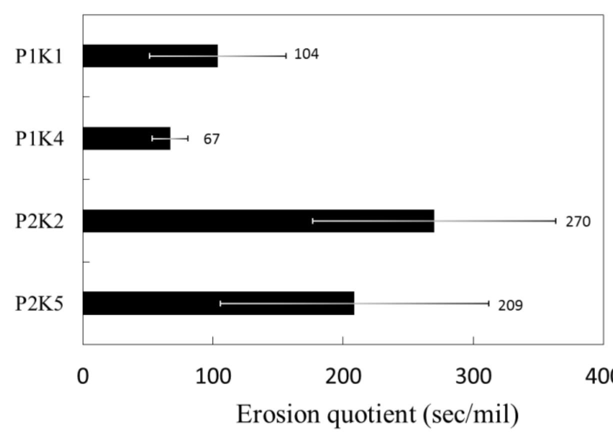

Figure 8: Erosion quotient – GKN Aerospace specifications

Corrosion Resistance

Samples were exposed to cyclic salt spray corrosive environment, and were inspected every week (every 160 hours), for a total exposure time of 6 weeks (1000 h). SEM micrographs of respective samples were taken (Fig 9) and pitting corrosion spots inspected (white arrows). Electrolytic hard chrome (EHC) sample exhibits corrosion spots likely occurring at pores and cavities in the coating as reported in literature (Ref 2), already after 4 weeks exposure (600 h). First pitting spots on both HVOF and HVAF WC-Co-Cr coatings appeared after 6 weeks exposure (1000 h). No pitting corrosion was observed for both WC-Co sprayed coatings.

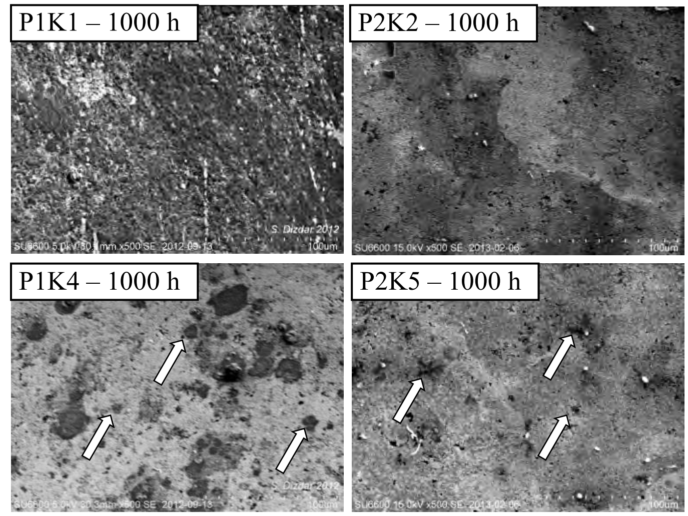

Figure 9: SEM micrographs (x500) of HVOF and HVAF coatings exposed to cyclic corrosion test after 1000 hours

More investigations are nevertheless required to evaluate the type of corrosion and how deep it occurs from the coated surface. Coatings surface finishing can as well influence corrosion results, and more care need to be addressed in the future about samples surface finishing in the aim of fulfilling industrial specifications for better comparison. More than correlating the porosity content and the difference in CGS and CC distributions to the respective coating wear and corrosion resistance, a first attempt has been here designed to evaluate as well the weighted distribution of the binder Mean Free Path (MFP). The number-weighted distribution of the distance between near-neighbour carbides is here presented (Fig 10), and preliminary studied utilizing a PeakFit Matlab® routine. However more work is required in order to compute the length-weighted distribution of the MFP relatively to the volume fraction of binder phase. This final step is about to be published in the extension of this work.

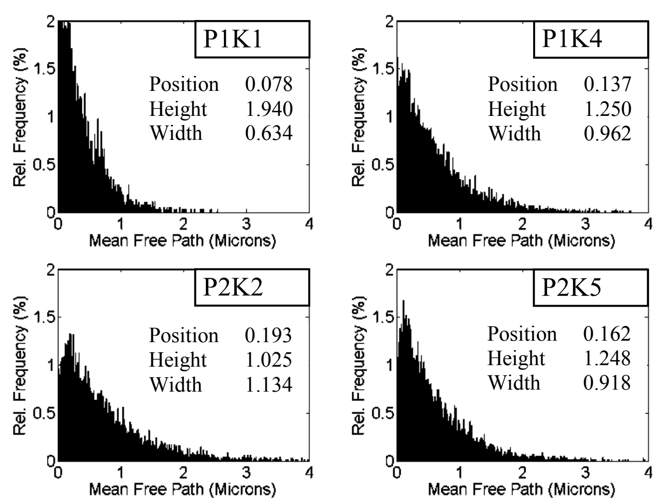

Figure 10: weighted distributions of Mean Free Path (MFP)

Conclusion

HVOF coatings show on one hand significantly higher dry wear resistance than HVAF coatings, owing to the presence of coarser primary carbides from the initial coarser powder cut. HVAF coatings exhibit lower porosity and finer well-distributed primary carbides, which on the other hand are expected to improve coatings sliding wear performances (Ref 19, 20), while performing for instance the intended ASTM G77. Respective wear mechanisms sollicited in those different tests are to be investigated in the future, in order to highlight the fact that there is a strong effect of the used wear test on the wear behaviour, and thus depending on the targeted application. Further work will investigate the critical role of CGS, CC and MFP respective weighted distributions on the oxidation and corrosive resistance of HVAF-sprayed coatings.

Acknowledgments

The authors would like to express their gratitude to the KK-funded Swedish program for support towards this research program in Hard Chrome Replacement alternative technologies. The authors wish to gratefully acknowledge the experimental assistance of GKN-Aerospace for erosion tests.

References

1. K.O. Legg, M. Graham, et al., The Replacement of Electroplating, *Surface and Coatings Technology* (81), pp. 99-105, 1996
2. K. Legg, J. Sauer, “Use of Thermal Spray as an Aerospace Chrome Plating Alternative”, Rowan Technology Group, Rowan Project # 3105JSF3, 2000
3. G. Bolleli, V. Cannillo, et al., Mechanical and Tribological Properties of Electrolytic Hard Chrome and HVOF-Sprayed Coatings, *Surface and Coatings Technology* (200), pp. 2995-3009, 2005
4. E. Bergonzini, G. Bolelli, et al., Wear Behaviour of HVOF-Sprayed Nanostructured WC-Co-Cr Coatings, *Proceedings of the International Thermal Spray Conference ITSC 2011*, pp. 612-618, 2011
5. E. Altuncu, F. Ustel, et al., Sliding Wear Behaviour of HVOF Sprayed Metal Matrix Carbides, *Proceedings of the International Thermal Spray Conference ITSC 2011*, pp. 485-488, 2011
6. G. Bolleli, R. Giovanardi, et al., Corrosion Resistance of HVOF-Sprayed Coatings for Hard Chrome Replacement, *Corrosion Science* (48), pp. 3375-3397, 2006
7. J.K.N. Murthy, B. Venkataraman, Abrasive Wear Behaviour of WC–CoCr and Cr3C2–20(NiCr) Deposited by HVOF and Detonation Spray Processes, *Surface and Coatings Technology*, 200, pp. 2642-2652, 2006
8. L. Fedrizzi, L. Valentinelli, et al., Tribocorrosion Behaviour of HVOF Cermet Coatings, *Corrosion Science* 49, pp. 2781-2799, 2007
9. A. Pelz, Analysis of Fe-Base Materials and Evaluation of their Suitability for Wear Protection Coatings, *Proceedings of the International Thermal Spray Conference ITSC 2010*, pp. 766-772, 2010
10. A. Määttä, U. Kanerva, et al., Structure and Tribological Characteristics of HVOF Coatings Sprayed from Powder Blends of Cr3C2-25NiCr and NiCrBSi Alloy, *Proceedings of the International Thermal Spray Conference ITSC 2010*, pp. 31-35, 2010
11. J.M. Guilemany, J.M. Paco, et al., Characterization of the W2C Phase Formed during the High Velocity Oxygen Fuel Spraying of a WC-12Co Powder, *Metallurgical and Materials Transactions, A*(30), pp. 1913-1921, 1999
12. Z.-G. Ban, L. L. Shaw, Characterization of Thermal Sprayed Nanostructured WC-Co Coatings Derived from Nanocrystalline WC-18wt.%Co Powders, *Journal of Thermal Spray Technology*, 12(1), pp. 112-119, 2001
13. P. Chivavibul, M. Watanabe, et al., Development of WC-Co Coatings Deposited by Warm Spray Process, *Journal of Thermal Spray Technology*, 17(5-6), pp. 750-756, 2008
14. P.L. Clavette, A. J. Nardi, et al., Erosion Resistance of WC-12Co High Velocity Oxy-Fuel Coatings, *Proceedings of the International Thermal Spray Conference ITSC 2011*, pp. 246-251, 2011
15. L.–M. Berger, S. Saaro, et al., Microstructure and Properties of HVOF-Sprayed WC-(W,Cr)2C-Ni Coatings, *Journal of Thermal Spray Technology* 17(3), pp. 395-403, 2008
16. L. Jacobs, M. Hyland, et al., Study of the Influence of Microstructural Properties on the Sliding-Wear Behavior of HVOF and HVAF Sprayed WC-Cermet Coatings, *Journal of Thermal Spray Technology* 8(1), pp. 125-132, 1999
17. E. Underwood, *Quantitative Stereology*, Addison-Wesly, Inc., New York, 1970
18. ASTM E562-11, Standard Test Method for Determining Volume Fraction by Systematic Manual Point Count
19. B. Wielage, A. Wank, et al., Development and Trends in HVOF Spraying Technology, *Surface and Coatings Technology* (201), pp. 2032-2037, 2006
20. J.M. Guilemany ,S. Dosta, J. Nin, J.R. Miguel, Study of the Properties of WC-Co Nanostructured Coatings Sprayed by High-Velocity Oxyfuel, Journal of Thermal Spray Technology 14(3), pp. 405-41, 2005